~~CONFIDENTIAL~~

ORNL MASTER COPY

OAK RIDGE NATIONAL LABORATORY
operated by
UNION CARBIDE CORPORATION
for the
U. S. ATOMIC ENERGY COMMISSION

ORNL - TM - 526

Classification Cancelled
[redacted]
By Authority Of TID 1380
By _____ Date SEP 13 1971

ISOTOPES DEVELOPMENT CENTER

PROGRESS REPORT

CURIUM PROGRAM

JANUARY 1963

SPECIAL REREVIEW FINAL DETERMINATION
CLASS. U AUTH. _____
REVIEWERS/VERIFIERS CLASS. DATE
(1) K. H. Baker U 7/31/80
(2) A. T. Gresky U 7/31/80

This material contains information affecting the national defense of the United States within the meaning of the espionage laws, Title 18, U.S.C., Secs. 793 and 794, the transmission or revelation of which in any manner to an unauthorized person is prohibited by law.

NOTICE

This document contains information of a preliminary nature and was prepared primarily for internal use at the Oak Ridge National Laboratory. It is subject to revision or correction and therefore does not represent a final report. The information is not to be abstracted, reprinted or otherwise given public dissemination without the approval of the ORNL patent branch, Legal and Information Control Department.

~~CONFIDENTIAL~~

LEGAL NOTICE

This report was prepared as an account of Government sponsored work. Neither the United States, nor the Commission, nor any person acting on behalf of the Commission:

A. Makes any warranty or representation, expressed or implied, with respect to the accuracy, completeness, or usefulness of the information contained in this report, or that the use of any information, apparatus, method, or process disclosed in this report may not infringe privately owned rights; or

B. Assumes any liabilities with respect to the use of, or for damages resulting from the use of any information, apparatus, method, or process disclosed in this report.

As used in the above, "person acting on behalf of the Commission" includes any employee or contractor of the Commission, or employee of such contractor, to the extent that such employee or contractor of the Commission, or employee of such contractor prepares, disseminates, or provides access to, any information pursuant to his employment or contract with the Commission, or his employment with such contractor.

[redacted]

ORNL-TM-526

Contract No. W-7405-eng-26

ISOTOPES DEVELOPMENT CENTER

PROGRESS REPORT

CURIUM PROGRAM

January 1963

Eugene Lamb, Isotopes Division

Prepared from Reports by:

F. T. Binford, Operations Division
T. A. Butler, Isotopes Division
D. E. Ferguson, Chemical Technology Division
R. A. Robinson, Isotopes Division
R. W. Schaich, Isotopes Division

DATE ISSUED

APR 19 1963

[redacted] contains information affecting the national defense of the United States within the meaning of the espionage laws, Title 18, U.S.C., Sections 793 and 794, the transmission or revelation of which in any manner to an unauthorized person is prohibited by law.

OAK RIDGE NATIONAL LABORATORY
Oak Ridge, Tennessee
operated by
UNION CARBIDE NUCLEAR COMPANY
for the
U. S. ATOMIC ENERGY COMMISSION

[redacted]

CONTENTS

1. Irradiation of Americium-241 1

1.1. Reactor Production-Rate Experiments 1

1.2. Calorimetric Determination of Curium-242. 4

1.3. Irradiation Target Fabrication. 5

1.4. Target Shipping Casks 6

2. Chemical Process Development 14

2.1. Tramex Flowsheet Test at High Power Density 14

2.2. Curium Recovery Facility. 15

3. Curium-242 Source Fabrication. 15

3.1. Chemical Process Development. 15

3.2. Source Fabrication Development. 17

3.3. Source Fabrication Facility (SFF) 19

3.4. Radiation Safety. 21

3.5. Generator Fueling 21

CURIUM PROGRAM

1. IRRADIATION OF AMERICIUM-241

1.1. Reactor Production-Rate Experiments

Five 100-mg AmO_2 samples were irradiated in the ORR and discharged on January 13, 1963. Irradiation and heat generation data on these samples are presented in Table 1.1.1.

Table 1.1.1. Basic Data on Five Irradiated AmO_2 Samples

Sample No.	Initial Am^{241} (as element) (mg)	Am^{241} Fissioned (mg)	Flux (Neutrons cm^{-2} sec^{-1})	Irradiation Time (days)	Total Heat Output (w)	Cm^{242} Heat Output (w)
E-9-9	80.9	7.4	3.49×10^{14}	62	3.91	3.7
E-10-1	82.4	6.6	3.49×10^{14}	50	3.72	3.5
E-11-1	81.3	6.5	3.49×10^{14}	50	3.71	3.5
F-1-1	106.6	8.5	3.49×10^{14}	50	4.64	4.3
F-2-1	78.2	6.3	2.58×10^{14}	50	3.37	3.1

The total heat output of each sample was measured calorimetrically and contains no correction for heating due to other radioisotopes. The weight of Am^{241} fissioned is calculated from practical cross section values, the flux, and the integrated flux.

The measured thermal power contains contributions by the fission products, residual Am^{241}, Pu^{238}, Cm^{243}, and Am^{242}. The major contribution during the first 60 days after reactor discharge is the heat produced by the short-lived fission products. The fission product heating, amounting to ~8% of the total heat output at the time of measurement, was calculated for each sample and subtracted from the total heat output to obtain the heat generated by the Cm^{242}. The heat contributed by Am^{241}, Am^{243}, Pu^{238}, and Pu^{242} combined amounted to $< 0.3\%$ and was neglected because this value is within the experimental error.

The corrected heat outputs were further adjusted for decay of Cm^{242} and converted to milligrams of Cm^{242} to obtain the percent conversion of Am^{241} to Cm^{242} at reactor discharge. The results are given in Table 1.1.2. These experimental values are 1% lower than the calculated values.

Table 1.1.2. Percentage Conversion of Am^{241} to Cm^{242} at Reactor Discharge

Sample	Am^{241} (mg)	Decay Factor	Corrected Heat Output (w)	Cm^{242} at Discharge (mg)	% Conversion Am^{241} to Cm^{242}
E-9-9	80.9	.986	3.723	30.9	38.2
E-10-1	82.4	.985	3.519	29.2	35.4
E-11-1	81.3	.980	3.532	29.3	36.0
F-1-1	106.6	.985	4.362	36.2	34.0
F-2-1	78.2	.981	3.194	26.5	33.9

The percentage of initial Am^{241} that fissions is strongly dependent on the integrated flux, and calculated values are given in Table 1.1.3 as a function of integrated flux (nvt) for three flux values.

Table 1.1.4 lists the calculated values of the residual Am^{241} as a percentage of the initial Am^{241} for various total integrated fluxes.

Table 1.1.3. Percentage of Am^{241} Fissioned as a Function of Flux and Irradiation Time

Irradiation Time (days)	1×10^{14}		2×10^{14}		3×10^{14}	
	nvt	%Am^{241} fissioned	nvt	%Am^{241} fissioned	nvt	%Am^{241} fissioned
10	8.64×10^{19}	0.10	1.73×10^{20}	0.60	2.59×10^{20}	1.31
20	1.73×10^{20}	0.55	3.46×10^{20}	1.53	5.18×10^{20}	2.77
30	2.59×10^{20}	0.87	5.18×10^{20}	2.32	7.78×10^{20}	4.00
40	3.46×10^{20}	1.24	6.91×10^{20}	3.17	1.04×10^{21}	5.15
50	4.32×10^{20}	1.56	8.64×10^{20}	3.85	1.30×10^{21}	6.00
60	5.18×10^{20}	2.03	1.04×10^{21}	4.40	1.56×10^{21}	6.76
70	6.05×10^{20}	2.19	1.21×10^{21}	4.98	1.81×10^{21}	7.35
80	6.91×10^{20}	2.51	1.38×10^{21}	5.60	2.07×10^{21}	7.85
90	7.78×10^{20}	2.80	1.56×10^{21}	5.90	2.33×10^{21}	8.26
100	8.64×10^{20}	3.50	1.73×10^{21}	6.30	2.56×10^{21}	8.68

Table 1.1.4. Percentage of Am^{241} Left as a Function of Total Integrated Flux

Irradiation Time (days)	nvt at 2×10^{14} Flux	% Residual Am^{241}
10	1.73×10^{20}	89.0
20	3.46×10^{20}	78.5
30	5.18×10^{20}	70.0
40	6.91×10^{20}	61.5
50	8.64×10^{20}	54.5
60	1.04×10^{21}	49.0
70	1.21×10^{21}	43.0
80	1.38×10^{21}	38.0
90	1.56×10^{21}	34.0
100	1.73×10^{21}	30.0
120	2.08×10^{21}	23.5

1.2. Calorimetric Determination of Curium-242

The thermal powers of two samples of irradiated Am^{241} obtained from the MTR were remeasured to determine if the thermal power of long-lived radioactive impurities would be apparent from the declining power rate of the samples.

The rate of temperature rise in a system of known heat capacity was utilized for the measurements. The calorimeter consisted of a tall cylindrical Dewar flask containing a known amount of water. The top of the flask was sealed by a large cork stopper which was penetrated by a stirrer shaft and a thermometer. To calibrate the calorimeter, the total active heat capacity was determined by measurement of the rate of temperature rise produced by a heater of accurately known wattage.

After calibration, the heater was removed and similar rates of temperature rise were determined using the Cm^{242} samples. The average of three measurements on each sample was 30.3 ±0.6 w for MND-1-1 and 29.6 ±0.6 w for MND-1-2.

Previous measurements of the heat generation rate of these samples made September 14, 1962, gave 52 ±2 w for both samples. The power on January 24, 1963, calculated from the earlier value and using a Cm^{242} half-life of 162.5 days, should have been 29.6 w. The close agreement of the later values with those calculated using the Cm^{242} decay rate indicates that only a small part of the sample heat comes from radioisotopes other than Cm^{242}.

1.3. Irradiation Target Fabrication

The design of the americium targets has been completed and Table 1.3.1 gives the specifications and reference photographs.

Table 1.3.1. Americium Target Data

Item	Specifications	Fig. No.
Pellets per capsule	12	1.3.4
Pellet dimensions	0.5 in. x 0.420 in. diam	1.3.3
Pellet sleeve wall thickness	0.040 in.	1.3.3
Pellet end cap thickness	0.070 in. top, 0.050 in. bottom	1.3.3
Pellet powder weight composition	72.3% Al (200 mesh) 27.7% AmO_2	-
Capsule material	Type 1100 aluminum, H14	-
Capsule dimensions	8 in. x 0.5 in. OD x 0.430 in. ID	1.3.4
Capsule bottom plug	0.1875 in. x 0.430 in. diam	1.3.4
Capsule top plug	0.1875 in. x 0.430 in. diam	1.3.4
Capsule spacer dimensions	1.25 in. x 0.420 in. OD x 0.290 in. ID	1.3.4
Total weight of Al per capsule	57.3 g	-
Total weight of AmO_2 per capsule	3.4 g	-
Target Assembly	Designed for 18 capsules	1.3.10

The target pellets are pressed at 40,000 psi (Fig. 1.3.1) and have densities of ~91% of theoretical. The loaded capsule is hydraulically collapsed (Fig. 1.3.7) around the pellets at 8000 psig to reduce the clearance between the pellets and capsule wall to 0.001 in. or less. Radiographs of eight welded capsules in Fig. 1.3.8 show that the required minimum clearance was achieved.

The free gas volume inside the capsule is 0.17 $in.^3$, which includes the free volume in the individual pellets resulting from the difference between actual and theoretical density as well as the gas volume provided by the capsule spacer.

Target Development

Four die assemblies were fabricated and ~15 simulated pellets were pressed. The dies and punches (Fig. 1.3.2) were cleaned in concentrated NaOH to

remove residual aluminum. The number of pellets that may be pressed with one die assembly varies from 4 to 8. Eventually, the long punch freezes in the die body and cannot be removed with the ejector punch.

A standard capsule was loaded (Fig. 1.3.5) with 13 pellets, 4 spacer discs, and one spacer tube, and sealed by welding (Fig. 1.3.6). The capsule was tested in ethylene glycol at 25 in. Hg vacuum and revealed no leaks.

During the swaging operation, the area around the spacer tube collapsed at 8000 psig. An examination of the capsule revealed a slight lengthwise ridge with approximate dimensions of 3 x 1/16 x 0.005 in. The clearance between the capsule and the pellets is estimated to be less than 0.0005 in. Additional capsules will be prepared with heavier walled spacer tubes to withstand the swaging pressure.

Although the capsule seal welds did not leak during the leak test, sectioned specimens were microphotographed and Fig. 1.3.9 indicates that gassing occurred during the welding operation. Future end plugs will be made with a small vent hole which will be sealed after the end plug is welded. Further experiments to perfect the welding, swaging and leak test operations will be conducted.

Table 1.3.2 indicates the progress to date on the design and fabrication phases of the project.

Table 1.3.2. Target Fabrication Equipment

Description	Design % Complete	Fabrication % Complete	Remarks
Blender	100	50	Testing of prototype model in progress
Press	100	100	Testing in progress
Pellet loading device	100	100	Testing in progress
Swaging tool	100	100	Testing in progress
Capsule	95	10	Testing in progress
Leak testing equipment	90	5	Criteria not complete

1.4. Target Shipping Cask

Drawings of the MND cask have been received, and the necessary revisions are 96% complete.

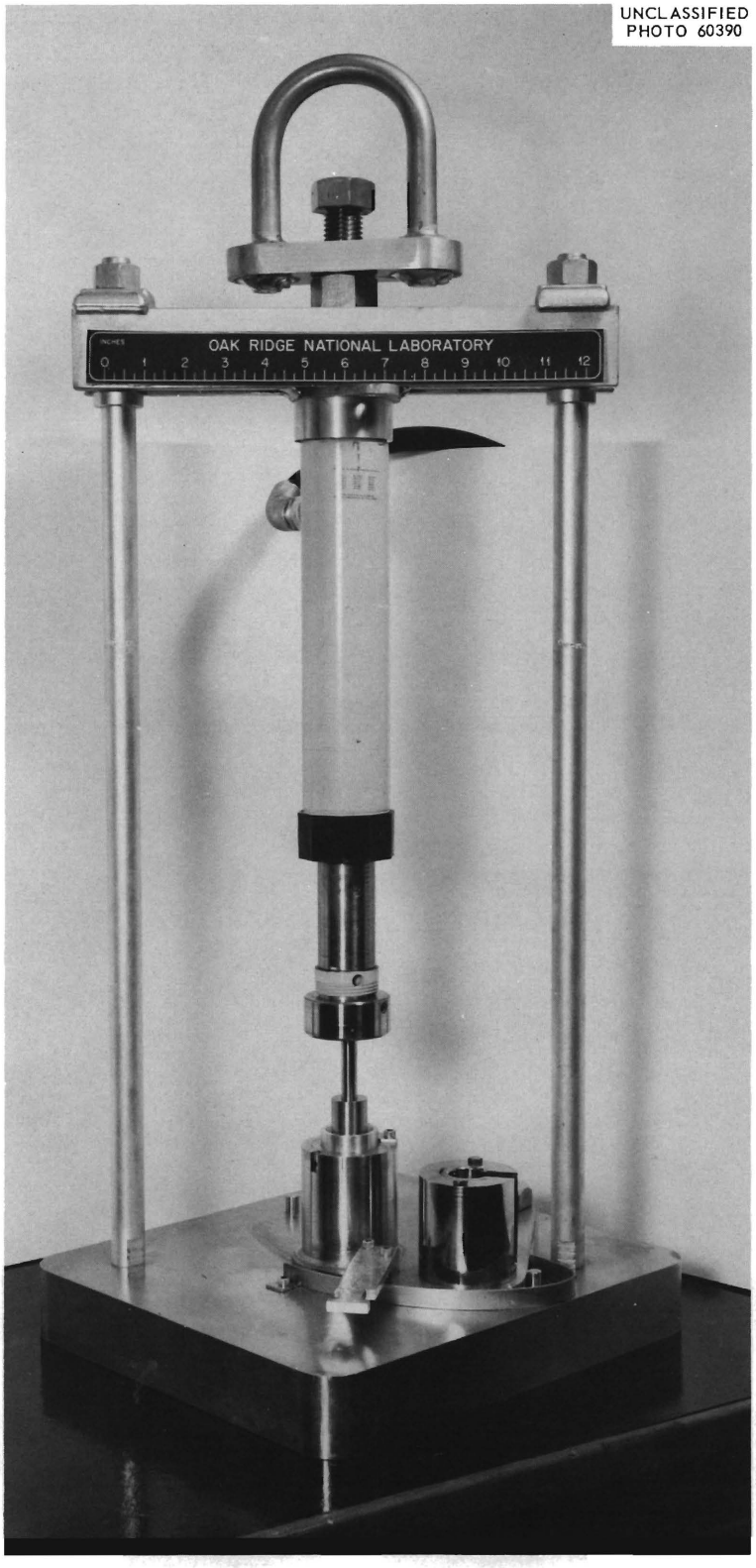

Fig. 1.3.1. Americium-241 Pellet Press

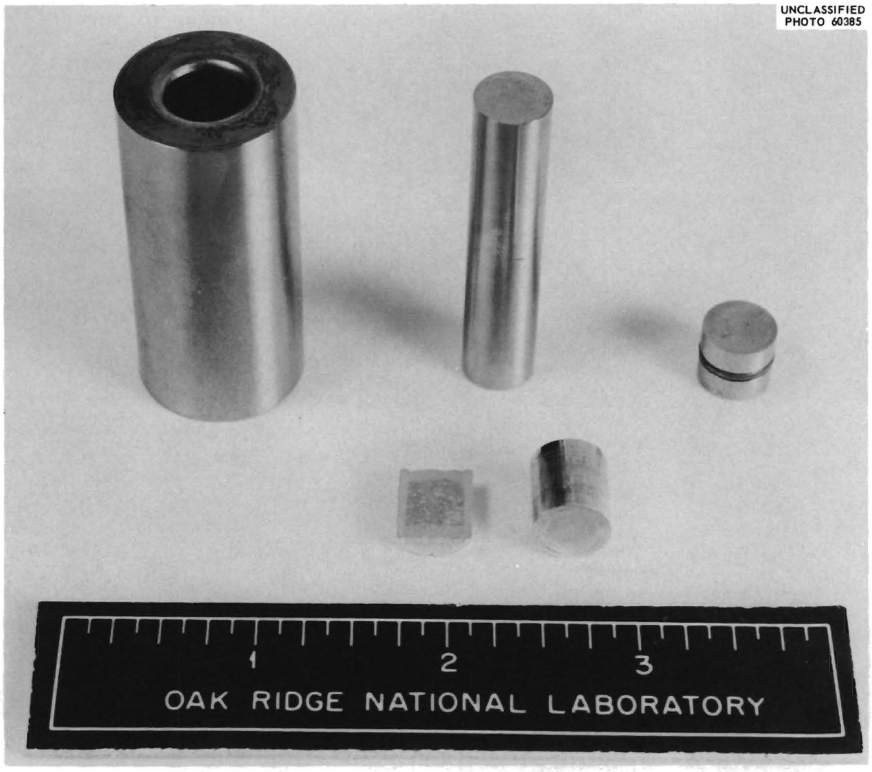

Fig. 1.3.2. Americium-241 Die Assembly and Pellets

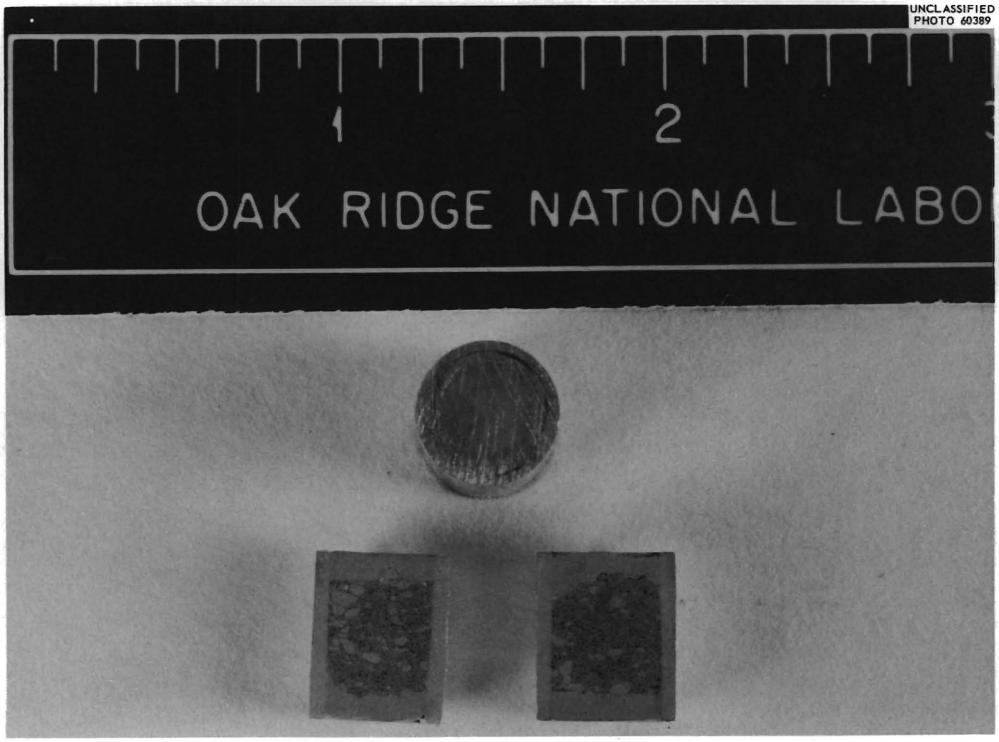

Fig. 1.3.3. Americium-241 Sectioned Pellets

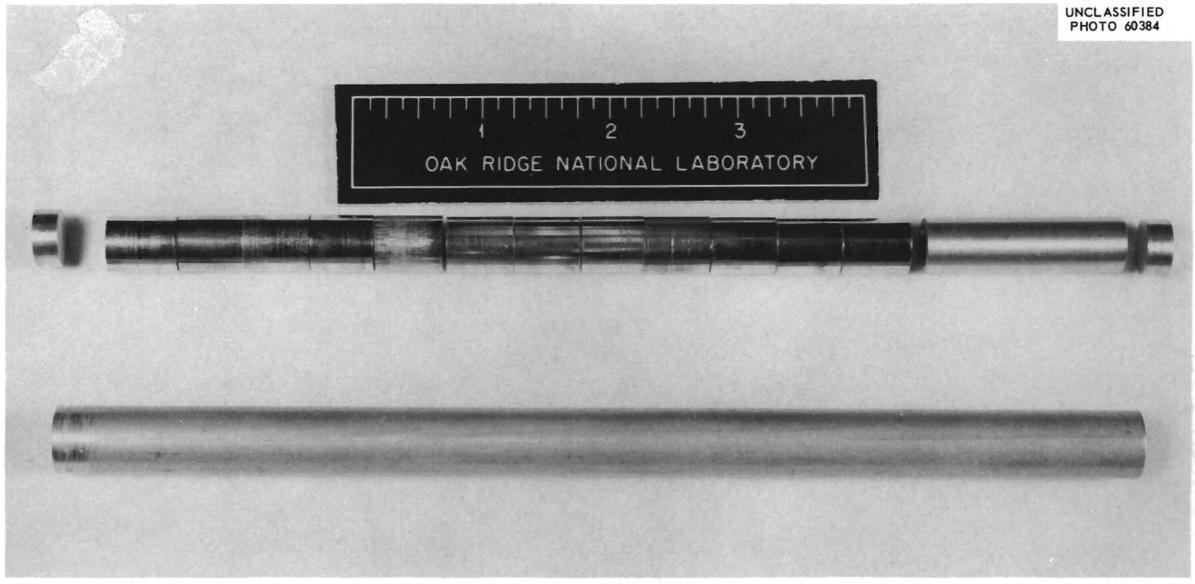

Fig. 1.3.4. Americium-241 Pellets, Spacer, End Plugs and Capsule

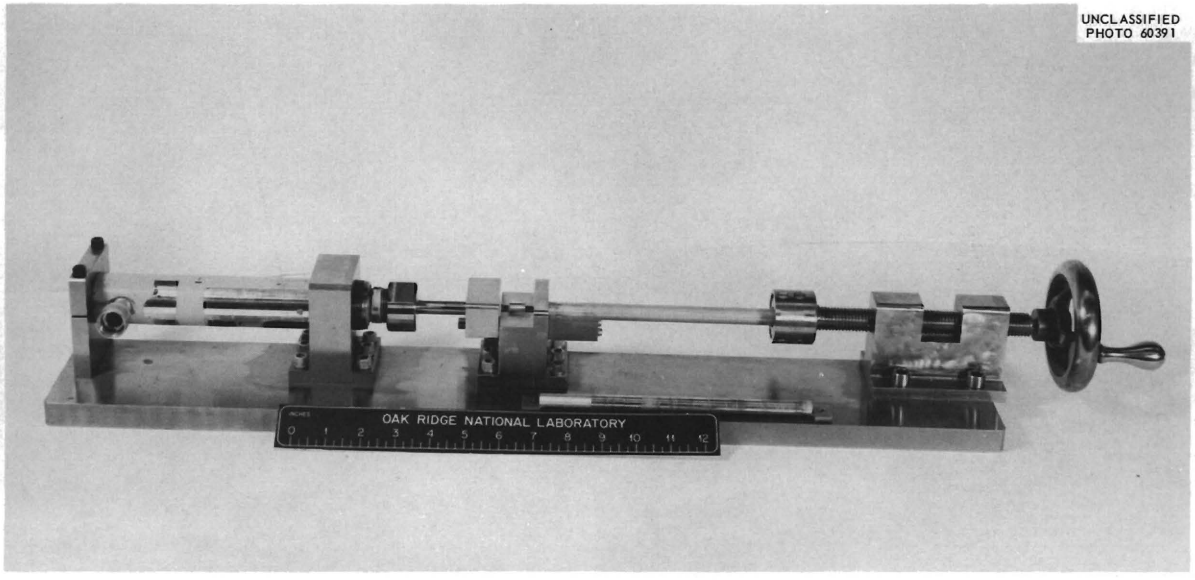

Fig. 1.3.5. Americium-241 Capsule Loading Device

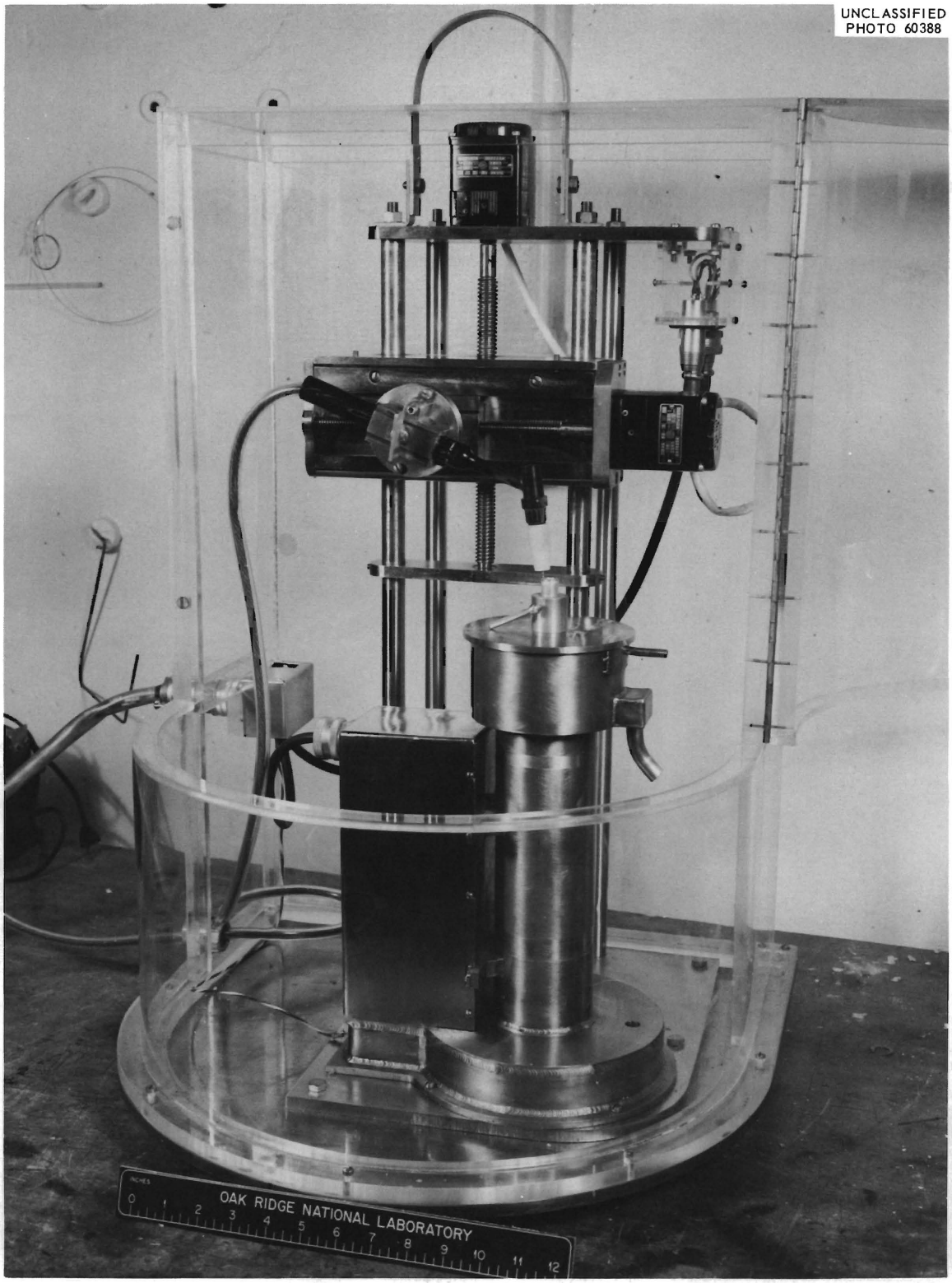

Fig. 1.3.6. Americium-241 Capsule Welder

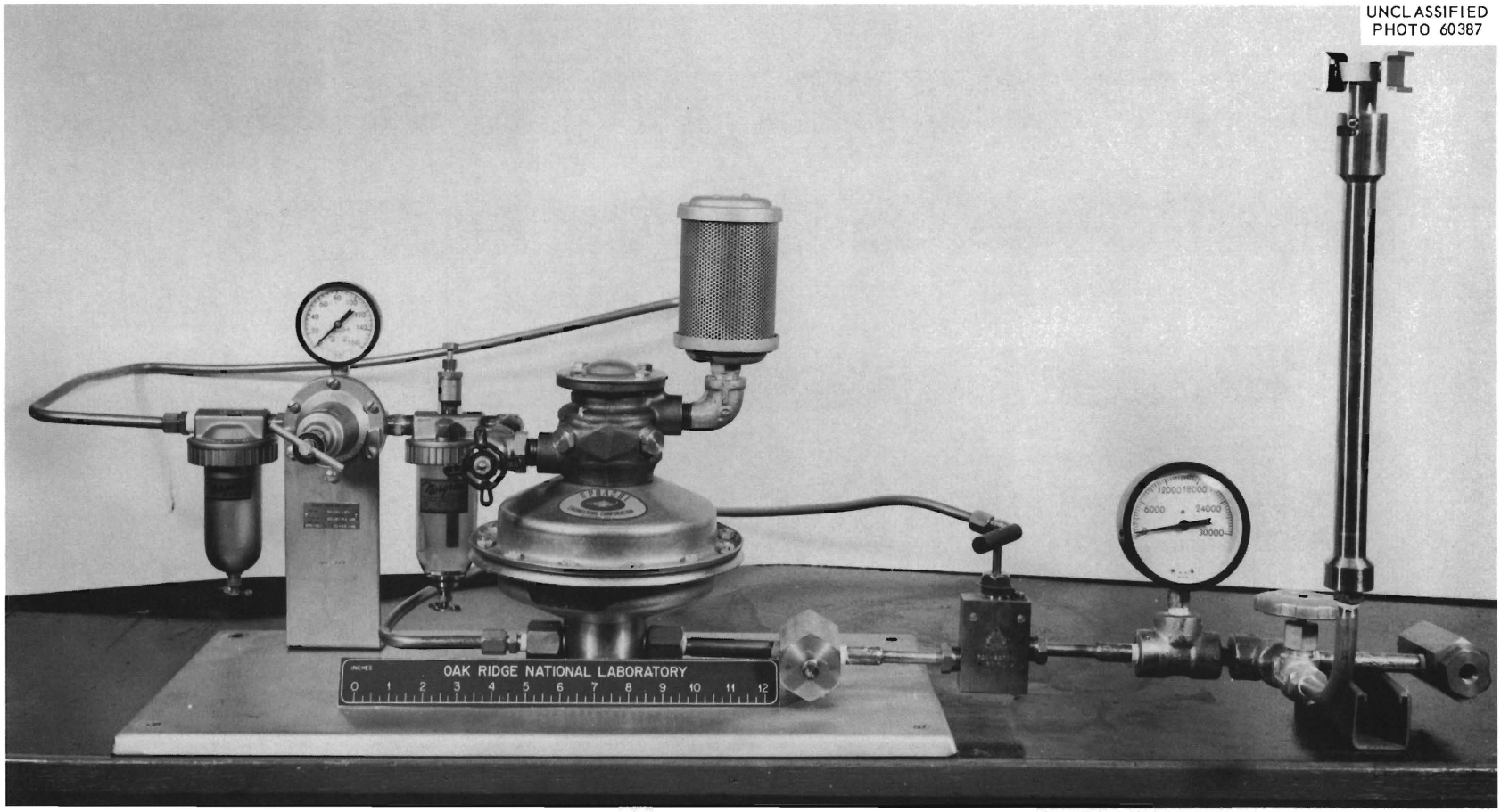

Fig. 1.3.7. Americium-241 Capsule Swaging Device

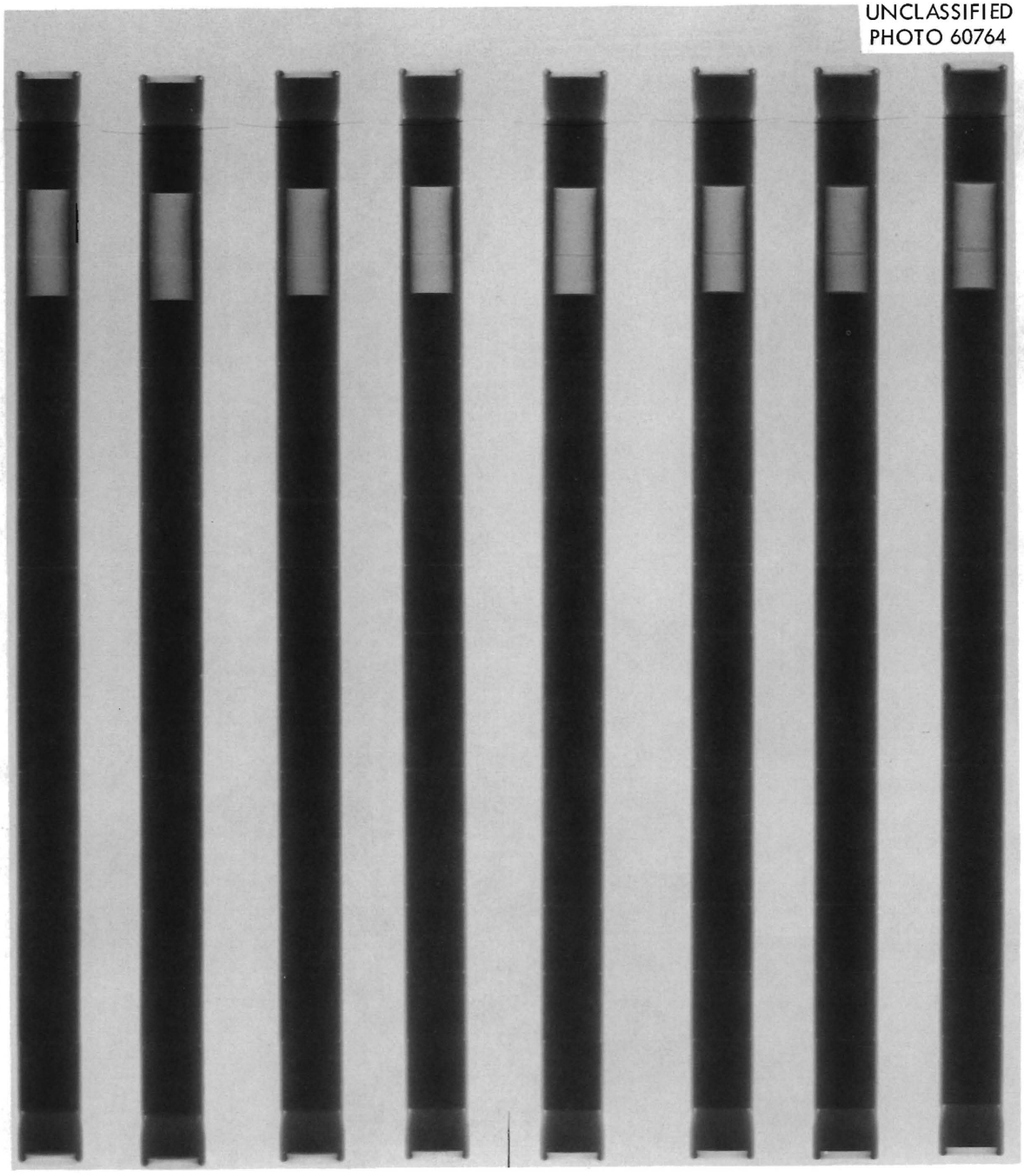

Fig. 1.3.8. Radiographs of Americium-241 Capsules

Fig. 1.3.9. Americium Target Capsule Weld

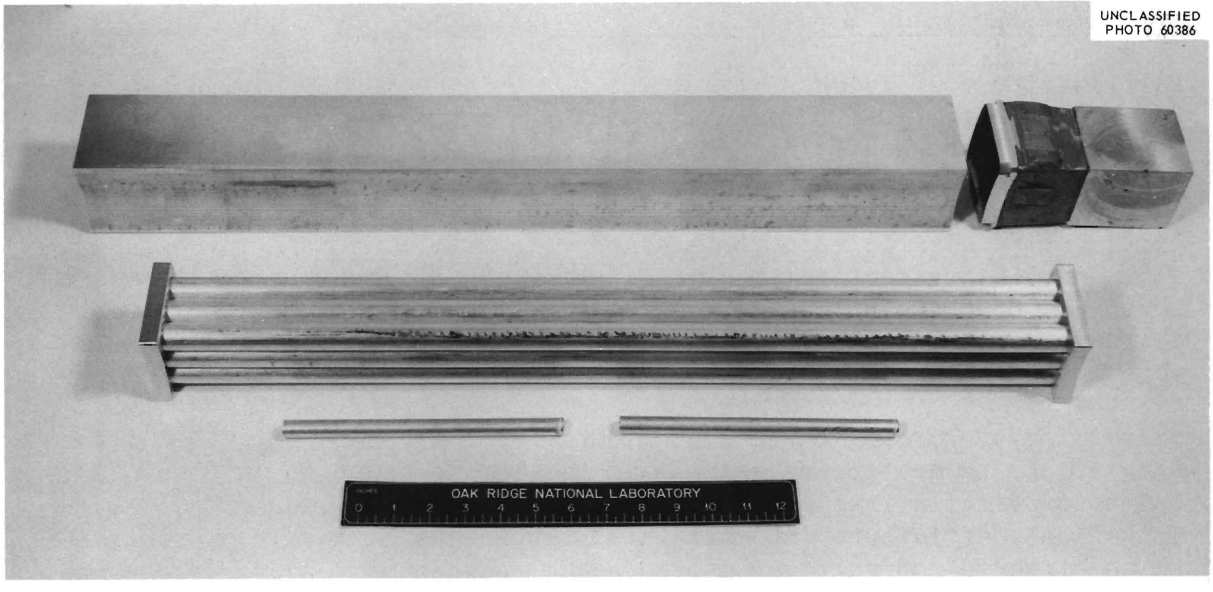

Fig. 1.3.10. Americium-241 Target Assembly

2. CHEMICAL PROCESS DEVELOPMENT

2.1. Tramex Flowsheet Test at High Power Density

The equipment for the second high-activity level test in the Analytical Hot Cells has been procured and is now being assembled in the alpha containment box. Four samples of irradiated Am^{241} will be discharged in February and March to provide Cm^{242} for the full-level Tramex tests.

Effect of Acid Concentration on Tramex Extraction

Distribution coefficients were determined for HCl between the hydrochloride salt of 0.6 M Alamine 336 in diethylbenzene and feeds containing 9, 10, and 11 M LiCl over an acid range of 0.01 to 2.0 M. The distribution coefficients of HCl for feeds containing 0.01 M HCl were 4, 9, and 20, respectively for 9, 10, and 11 M LiCl. Distribution coefficients decreased with increasing acid concentration.

The effect of acid on europium distribution coefficients over the above acid range was determined for 9 and 10 M LiCl feeds. Europium distribution coefficients from 9 M LiCl decreased from 0.005 to 0.0004 as the free acid concentration in the solvent increased from 0.02 to 0.2 M. With 10 M LiCl, europium distribution coefficients decreased from 0.012 to 0.0012 as the free acid concentration in the solvent increased from 0.03 to 0.3 M.

These studies will be extended to the effect of acid on americium extraction. The results will determine how much free acid can be tolerated in Tramex feed solutions.

Actinide-Lanthanide Separations in Carbonate Solutions

Distribution coefficients of americium, cerium, and europium between Dowex 21K resin (50-100 mesh) and $NaHCO_3$ solutions were inversely proportional to the $NaHCO_3$ concentration over the range 0.02 to 0.2 M. At lower concentrations there was a decrease in this dependency, perhaps as a result of rare earth and americium insolubility. At 0.1 M $NaHCO_3$, distribution coefficients for americium, cerium, and europium were 50, 110, and 350, respectively. Distribution coefficients between Dowex 21K resin and K_2CO_3 solutions increased slightly as the K_2CO_3 concentration increased from 0.02 to 0.2 M. At 0.1 M K_2CO_3, distribution coefficients were 100 for americium and 300 for europium.

Extraction of rare earths and americium from carbonate solutions into Aliquat 336 (a quaternary amine) was similar to sorption on Dowex 21K, but no extraction into Alamine 336 (a tertiary amine) was noted. Distribution coefficients into Aliquat 336 were approximately proportional to the inverse fourth power of the $NaHCO_3$ concentration over the range 0.25 to 1 M and to the inverse first power of the $NaHCO_3$ over the range 0.1 to 0.2 M. Separation factors decreased with increasing $NaHCO_3$

concentration. At 0.1 M $NaHCO_3$, americium, cerium, and europium distribution coefficients into 30% Aliquat 336-diethylbenzene were 20, 40, and 200, respectively. Extraction from K_2CO_3 solutions was similar in behavior but about a factor of two less for the same molarities of $NaHCO_3$ and K_2CO_3.

These results do not give positive indication that an actinide-lanthanide group separation is possible in the Aliquat 336-carbonate system. It seems probable that curium and heavier actinides will be more extractable than americium and will have distribution coefficients approaching or greater than those for cerium. Additional investigation is needed to resolve this and other questions concerning this system.

2.2. Curium Recovery Facility

The design of process equipment and cell alterations is 98% complete. The design of the roof area sample handling equipment is being checked and pipe details for prefabrication are 75% complete. Details of the sampling systems and shielding for the multichannel gamma spectrometer have not been started.

The construction of the makeup area is complete except for the installation of the glove box containing the pump drive. The operating area construction is complete except for the installation of the fire protection system and the gamma spectrometer equipment. The roof area equipment has not been installed, but all components except the sample removal box have been fabricated. All structural supports are in the cell, and installation of the piping has begun.

The plated cell tanks are at Parma, Ohio, being prepared for application of the tantalum. A tantalum valve is being fabricated in ORNL shops. When completed, this valve will be tested at the TRU mockup for operability and leakage.

3. CURIUM-242 SOURCE FABRICATION

3.1. Chemical Process Development

Zirconium Chemistry

The results of the Cm^{242} run previously reported[1] indicated that the separation of Zr-Nb from Cm^{242} by oxalate precipitation is low. Higher decontamination factors for Zr-Nb cannot be readily achieved because of the following requirements:

1. The oxalate solution is adjusted to pH 1-2 to minimize Cm^{242} losses due to solubility in solutions containing a high concentration of acid.

[1] E. Lamb, Curium Program December 1962, ORNL-TM-503

2. Zirconium tends to precipitate as a polynuclear complex in neutral or slightly acid solutions.

3. The presence of a considerable excess of complexing agent such as oxalate does not keep zirconium in solution.

4. The curium oxalate precipitate is dissolved in 4 N HNO_3, and the colloidal zirconium goes into solution under these conditions. The cycle is completed by decreasing the pH of the solution to reprecipitate curium oxalate.

The absorption of Zr-Nb by silica gel from 2 N and 4 N HNO_3 solutions was investigated as a means of separating Zr-Nb from curium. A volume of 50 ml of silica gel was preconditioned with HNO_3 and two 110-ml batches of HNO_3, 2 N and 4 N respectively, containing 40 mg/liter of zirconium were run through the column. The absorption of Zr-Nb by the silica gel column was 97.7% from the 2 N HNO_3 and 99.1% from the 4 N HNO_3 solution.

The effect of radiation generated H_2O_2 on the absorption of Zr-Nb by silica gel was examined by using a 10-ml silica gel column which was preconditioned with 4 N HNO_3. A volume of 110 ml of 4 N HNO_3 containing 40 mg/liter of zirconium and Zr^{95}-Nb^{95} tracer without H_2O_2 was passed through the column. The break-through of activity into the column effluent was followed as a function of the number of column volumes of solution put through the column. The instantaneous activity in the effluent is given as a percentage of the tracer activity in the initial solution. The results are shown in Table 3.1.1.

Table 3.1.1. The Percentage of Zr-Nb Activity in the Effluent versus the Number of Column Volumes

Column Volumes 4 N HNO_3	% Original Activity
2	3.8
3	8.6
4	8.9
5	9.7
6	9.9
8.5	8.3
10	8.9

About 90% of the initial Zr-Nb activity was absorbed by the silica gel from the 4 N HNO_3 solution. Hydrogen peroxide was added to make the solution 0.02 M in H_2O_2 and the experiment was repeated to simulate the effects of radiation on aqueous solutions. It was found that 66.3% of the Zr-Nb activity came through on the first column volume, and 86.1% of the Zr-Nb activity broke through on the second column volume. The H_2O_2 complexed most of the Nb^{95} and considerable amounts of Zr^{95}.

The precipitation of zirconium from 4 N HNO_3 as zirconium phosphate is being investigated. If this step is feasible, it could be performed in the presently planned equipment.

Buildup of Noncondensable Gas Above a Curium-242 Solution

A volume of 120 ml of 4 N HNO_3 solution containing 87.9 curies of Cm^{242} was placed in a 250-ml polyethylene bottle. The free space above the solution was 162 ml. A Magnahelic gauge was attached to the polyethylene bottle and a linear increase in pressure with time was observed. The observed pressure rise was 0.071 in. of water per minute from which the gas production rate was calculated to be 1.74 ml per hour per 100 curies of Cm^{242}.

3.2 Source Fabrication Development

Brazing Studies

The investigation of techniques for brazing a Gd_2O_3-Rh cermet to a tungsten plate has been continued. The sintering of the pellet and bonding it to the tungsten plate in one heating operation was first considered. A small Gd_2O_3-Rh pellet was sintered at temperatures > 1650°C on a tungsten plate. Figure 3.2.1 shows an enlargement of the interface between the sintered pellet and the tungsten plate. A metal bond was made between the rhodium of the pellet and the tungsten plate and no Gd_2O_3 was within 0.001 in. of the tungsten plate.

Further experiments have shown the undesirability of sintering the pellet and bonding it to the tungsten plate at the same time. When the two operations are carried on concurrently, the outer edge of the pellet bonds to the tungsten plate before the pellet has completely shrunk and the pellet then deforms on further sintering.

The use of palladium metal as a braze material was investigated by heating a cermet pellet-palladium sheet-tungsten plate sandwich to 1580°C. Figure 3.2.2 shows that the palladium metal diffused into the cermet and made a metallic bond with the tungsten plate. When a specimen of soft material is bonded to a hard material and then polished, the soft material erodes faster than the hard material, and an indentation of the soft material is left at the interface. The black line on Figure 3.2.2 is the shadow of the higher edge of tungsten metal on the lower palladium section. The metal bond of the cermet to the tungsten plate is excellent and no void areas are visible.

Gadolinium Oxide-Rhodium Cermet

The effect of contaminants in the feed powder of a Gd_2O_3-Rh cermet was extended with the study of the additions of Al_2O_3 and ZrO_2 in the amount of 1% of the Gd_2O_3-Rh mixture, respectively. The pellets were sintered at 1725°C for 2 hr in the Rh-Pt resistance furnace. Figure 3.2.3 shows an enlargement of the surface of the cermet with the Al_2O_3 addition. The crystals of Al_2O_3 are distinguishable from the white rhodium metal, the gray Gd_2O_3, and the black void spaces. The ZrO_2 contaminated cermet shows a similar pattern. The additions of either Al_2O_3 or ZrO_2 had no adverse effect on the final cermet.

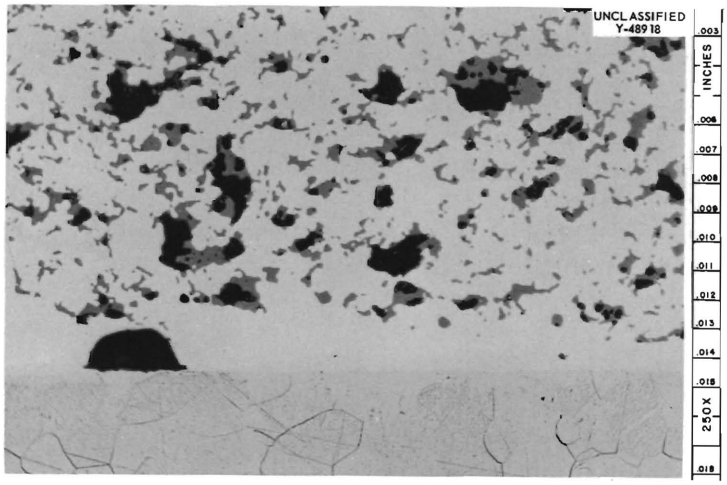

Fig. 3.2.1. Gd_2O_3-Rh Cermet Sintered to Tungsten. Reduced 40%.

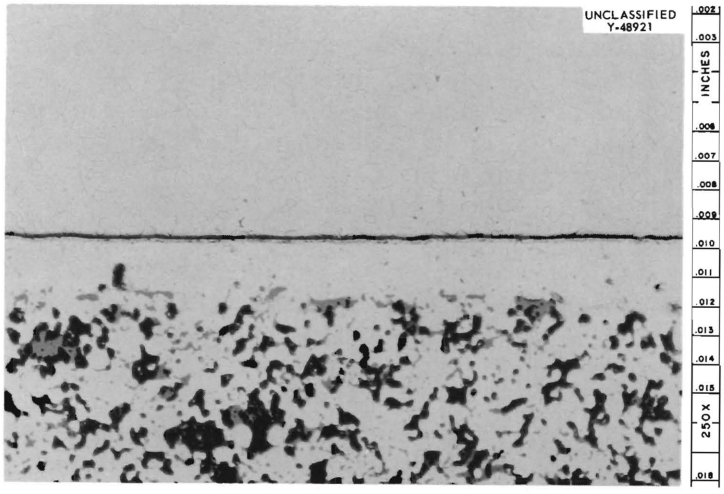

Fig. 3.2.2. Gd_2O_3-Rh Brazed to Tungsten with Paladium. Reduced 40%.

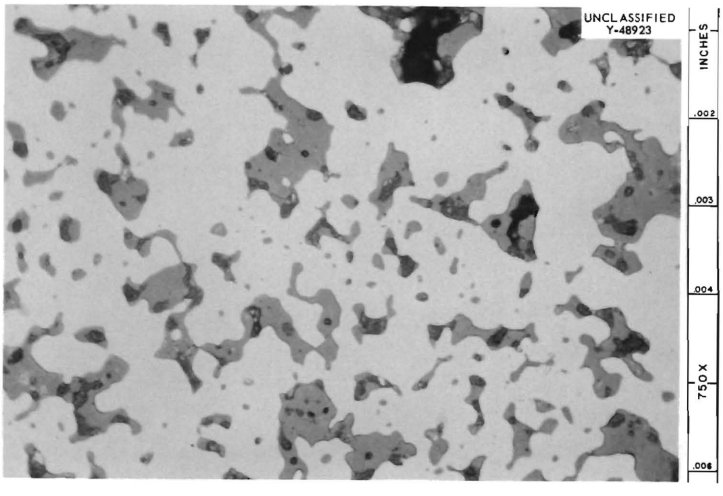

Fig. 3.2.3. Gd_2O_3-Rh Cermet with 1% Al_2O_3. Reduced 40%.

Sintering Furnace Development

A preliminary design of a vertical model of the graphite resistance furnace has been completed and is shown in Figure 3.2.4. The graphite heating element (1), which is shown partially lowered, connects electrodes (2) and (3) during furnace operation and retracts to permit access to the hot area. The graphite heating element is replaceable if an element is fractured. The electrodes are water cooled (4) to prevent overheating. The bell jar may be evacuated through the vacuum line (5) or operated under a helium atmosphere with a helium purge. The temperature of the pellet can be determined by an optical pyrometer through an observation hole (6) in the graphite element. The stabilized zirconia stand (7) is used to hold the pellet (8) for the sintering operation.

This vertical model has several advantages over the earlier reported horizontal experimental furnace. First, a uniform heating of the pellet is expected due to a longer heating element and the orientation of the pellet with respect to the furnace heating element. Second, this furnace will provide better containment of radioactivity and occupy less floor space than the horizontal model. A prototype of this furnace is under construction.

3.3 Source Fabrication Facility (SFF)

The structural modifications to the SFF building are ~45% complete. The preliminary proposal for the SFF equipment was transmitted to the AEC and proposal approval is expected by February 8, 1963.

The design status for the SFF and its equipment is indicated in Table 3.3.1 and Table 3.3.2, respectively.

Table 3.3.1. SFF Design Status

Description	% Complete
Structural	90
Piping	80
Air Handling	70
Electrical	90
Civil engineering	10
Cell ventilation	50
Cubicle No. 1 equipment layout	10
Feed transfer station	20

UNCLASSIFIED
ORNL-LR-DWG 78180

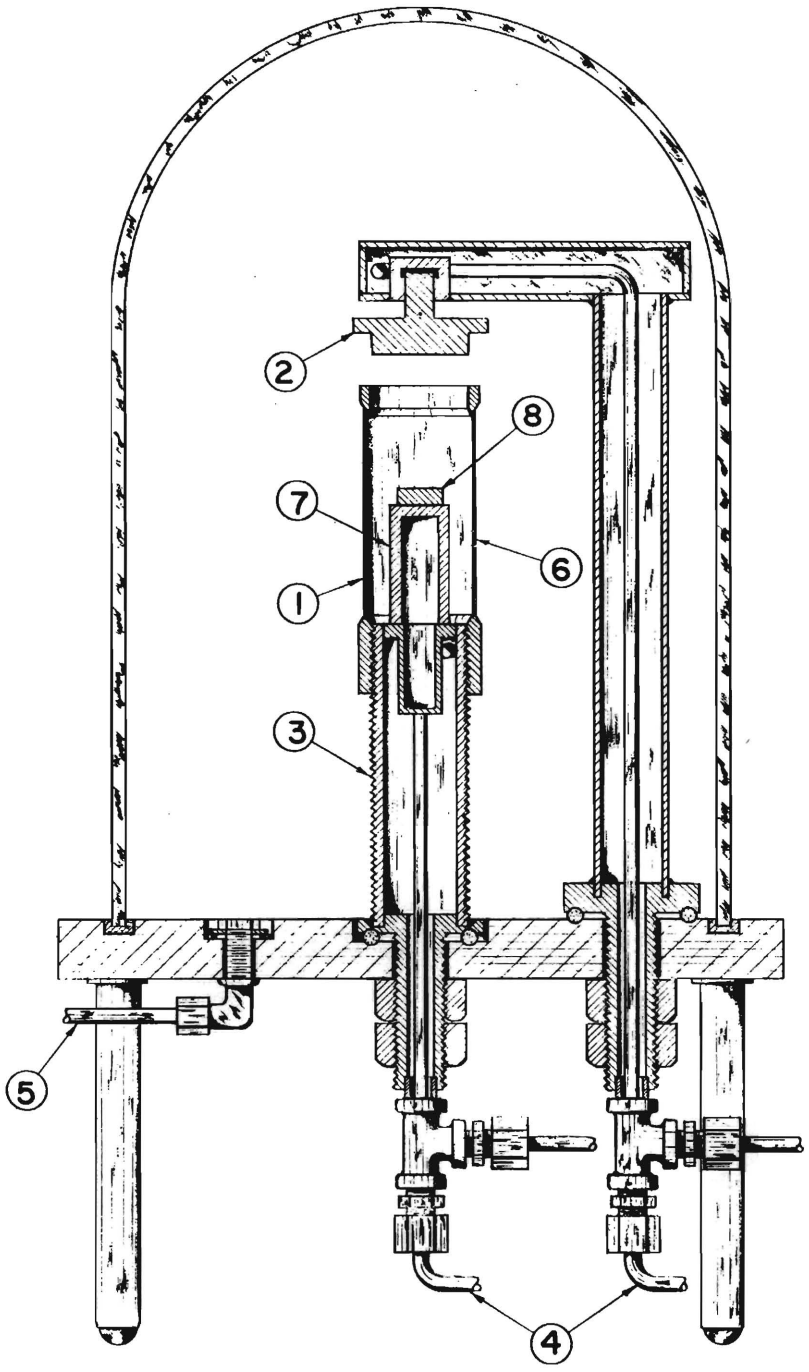

Fig. 3.2.4 Vertical Model of Graphite Resistance Furnace

Table 3.3.2. SFF Equipment Design Status

Description	% Complete
Bag-out port	98
Access port	98
Waste cask	95
Dolly	97
Sample cask	95
Manipulator decontamination	90
Welders	30
Doors and inter-cell transfers	50
Maintenance enclosure	10
Chill blocks	0
Cm^{242} press	0

3.4. Radiation Safety

The revised Radiation Safety Criteria were established at a meeting on January 25, 1963. Tentative agreement was reached with Radiation Safety and Control personnel on all proposed changes.

3.5. Generator Fueling

A review of the SNAP-13 fueling fixture was held at ORNL on January 25, 1963, with representatives from MND and the AEC present.

The design drawings for the fixture were transmitted to ORNL and a verbal description of the operations was presented by MND. Tentative agreement on all phases of the operations was reached by ORNL and MND, but ORNL will review design prints in detail before final verification.

A decision was made to use a cell in the ORNL Radioisotope Development Laboratory for the fueling operation since the unit requires a minimum of 5 ft from cell floor to fixture base plate. Composite drawings of the cell have been transmitted to MND.

DISTRIBUTION

1. F. T. Binford
2. W. D. Burch
3. F. L. Culler
4. D. E. Ferguson
5. E. Lamb
6. R. E. Leuze
7. A. F. Rupp
8-10. Laboratory Records
11. Laboratory Records - RC
12-13. Central Research Library
14. Document Reference Section
15-29. DTIE

EXTERNAL DISTRIBUTION

30. P. C. Aebersold, AEC, Washington, D. C.
31. Arnold Berman, AEC, Washington, D. C
32. R. T Carpenter, AEC, Washington, D. C.
33. James Cline, AEC, New York Operations Office, New York, N.Y.
34. D. C. Davis, AEC, ORO, Oak Ridge, Tennessee
35. W. K. Eister, AEC, Washington, D. C.
36-38. E. E. Fowler, AEC, Washington, D. C.
39. Eugene Giberson, Jet Propulsion Lab., California Inst. of Tech.
40-42. D. G. Harvey, Martin Company, Baltimore, Md.
43. Benjamin Milwitzky, National Aeronautics and Space Administration, Washington, D. C.
44-46. H. F. Prochaska, Hughes Aircraft Co., Culver City, Calif.
47. H. M. Roth, AEC, ORO, Oak Ridge, Tennessee
48. W. J. Lindsey, AEC, Washington, D. C.
49. W. P. Overbeck, SRL, E. I. DuPont, Aiken, S. C.
50. R. C. Blair, Attn: C. D. Bastin, SROO, AEC, Aiken, S. C.